

THE LINAC COHERENT LIGHT SOURCE (LCLS) ACCELERATOR*

Juhao Wu[†], P. Emma, SLAC, Menlo Park, CA 94025, USA

Abstract

The Linac Coherent Light Source (LCLS) is a SASE x-ray Free-Electron Laser (FEL) based on the final kilometer of the Stanford Linear Accelerator. Such an FEL requires a high energy, high brightness electron beam to drive the FEL instability to saturation. When fed by an RF-photocathode gun, and modified to include two bunch compressor chicanes, the SLAC linac will provide such a high quality beam at 14 GeV and 1- μm normalized emittance. In this paper, we report on recent linac studies, including beam stability and tolerances, longitudinal and transverse feedback systems, conventional and time-resolved diagnostics, and beam collimation systems. Construction and installation of the injector through first bunch compressor will be completed by December 2006, and electron commissioning is scheduled to begin in January of 2007.

INTRODUCTION

The LINAC Coherent Light Source (LCLS) will be the world's first x-ray Free-electron Laser (FEL) with a Self-Amplified Spontaneous Emission operation mode. It utilizes the last one third of the Stanford Linear Collider (SLC) accelerator system with a new injector and an 150 meter long undulator [1]. An x-ray FEL (XFEL) is possible only by a high brightness electron bunch. Such a high quality electron bunch should satisfy the following requirements. For the transverse phase space, its normalized emittance ϵ_n has to be small, $\epsilon_n \sim \gamma \frac{\lambda_r}{4\pi}$, where γ is the Lorentz factor of the electron and λ_r is the FEL radiation wavelength. For our case with parameters in Table 1, it then requires $\epsilon_n \sim 1 \mu\text{m}$. Similarly, for the longitudinal phase space, the rms relative energy spread σ_δ of the electron bunch should also be small, $\sigma_\delta \sim \rho \approx \frac{1}{4} \left[\frac{1}{2\pi^2} \frac{I_{pk}}{I_A} \frac{\lambda_w^2}{\beta \epsilon_n} \left(\frac{K}{\gamma} \right)^2 \right]^{1/3}$, where ρ is the pierce parameter, I_{pk} is the electron bunch peak current, $I_A \approx 17 \text{ kA}$ is the Alfven current, β is the β -function in the undulator, and K is the undulator parameter. With a $\beta = 18 \text{ m}$, and parameters in Table 1, we find the stringent requirement of $\sigma_\delta < 5 \times 10^{-4}$. Some of the key parameters for the electron bunch, the undulator, and the FEL performance are listed in Table 1. The notations have the following meaning. For the electron bunch, the energy is E , peak current I_{pk} , the normalized emittance ϵ_n , rms relative energy spread σ_δ , and rms bunch duration σ_t . The undulator has a period of λ_w , the undulator parameter K , and saturation length L_{sat} . The undulator length is actually total of 150 meters, and since $L_{sat} = 87 \text{ meters}$, the FEL runs into

deep saturation to reduce the power fluctuation. In Table 1, the FEL has a resonant wavelength of λ_r , peak power P_{pk} , power gain length L_G , effective pierce parameter ρ_{eff} , radiation peak brightness B_{pk} , radiation average brightness B_{ave} , rms power fluctuation $\sigma_{\Delta P/P}$, coherent length L_{coh} , and rms bandwidth $\sigma_{\Delta\omega/\omega}$.

Currently, the driving Laser for the RF-photocathode gun has been successfully installed. The first UV light has been generated. Place has been cleared in the research yard and construction has started. The electron commissioning is plan to start January 2007. A time-line for the construction, installation, and electron and FEL commissioning is shown in Fig. 1. The focus of the immediate following step is the commissioning of the RF-gun, injector, and up to the first bunch compressor (BC1). Magnets and solenoids are being tested in the newly opened Magnet Measurements Facility (MMF).

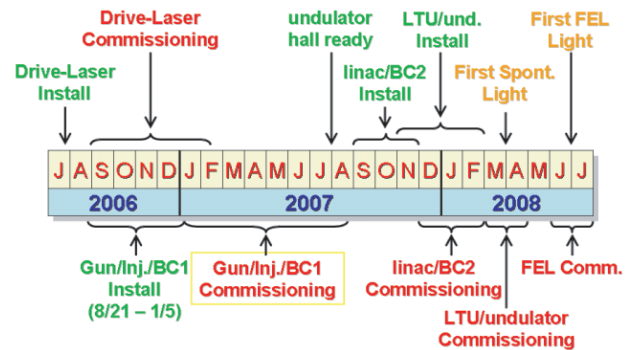


Figure 1: The time-line for LCLS construction, installation and electron / FEL commissioning.

The LCLS RF-Gun is shown in Fig. 2. It has a new design to allow normal incidence laser on the cathode. Previously, it was designed to be grazing incidence. With a normal incidence, a non-dispersed beam is possible. It also allows continuous variation of the cathode beam size. The integrated LCLS gun assembly with the diagnostic YAG screen and the energy spectrometer dipole is shown in Fig. 3, where the parameters for the RF-gun are also listed.



Figure 2: The LCLS RF-Gun.

* Work supported by the U.S. Department of Energy under Contract No. DE-AC02-76SF00515.

[†] jhwu@SLAC.Stanford.EDU

Table 1: Parameters for the electron bunch, the undulator, and the FEL performance.

Electron bunch						Undulator		
E (GeV)	I_{pk} (kA)	ϵ_n (μm)	σ_δ	σ_t (fs)	f (Hz)	λ_w (cm)	K	L_{sat} (m)
13.6	3.4	1.2	1×10^{-4}	77	120	3	3.5	87

FEL performance								
λ_r (\AA)	P_{pk} (GW)	L_G (m)	ρ_{eff}	B_{pk}^1	B_{ave}^2	$\sigma_{\Delta P/P}$ (%)	L_{coh} (nm)	$\sigma_{\Delta\omega/\omega}$
1.5	9	4.8	2.93×10^{-4}	0.8×10^{33}	4×10^{22}	6	25	12×10^{-4}

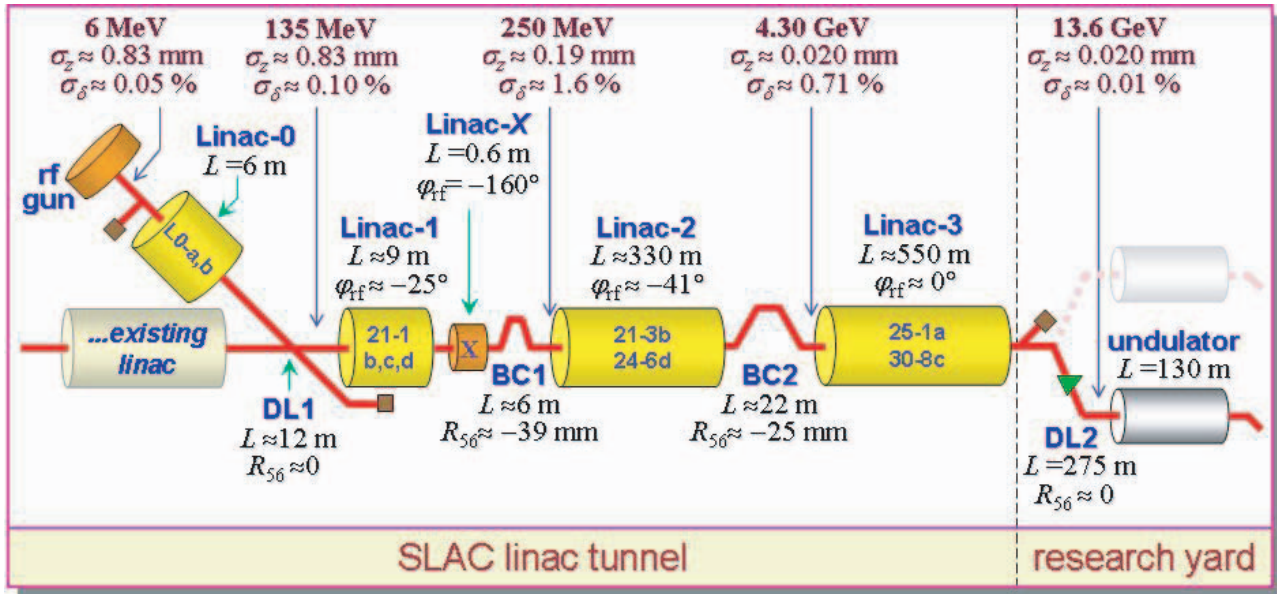


Figure 4: The LCLS accelerator and compressor system.

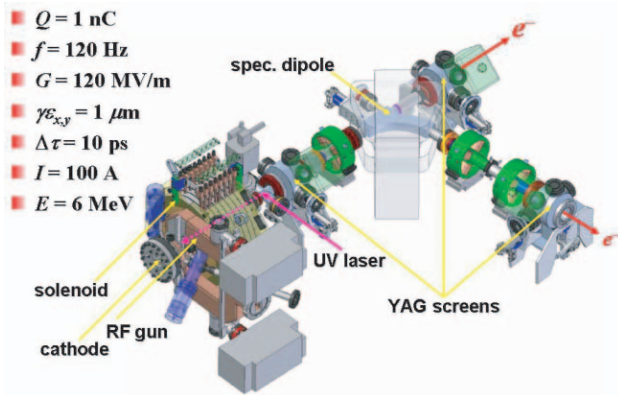


Figure 3: The LCLS-gun with diagnostics.

The LCLS accelerator and compressor system are shown in Fig. 4. There will be two bunch compressors (BCs). The first one, BC1, will be installed at an electron energy $E = 250$ MeV. The BC1 compresses the electron bunch rms bunch length from $\sigma_z = 830 \mu\text{m}$ to $\sigma_z = 190 \mu\text{m}$. This is achieved by off-peak acceleration to introduce a correlated energy spread in the electron beam, which can be compressed when it passes through the dispersive chicane. The detailed parameters for the accelerator amplitude and phase are given in Fig. 4. Due to the relatively long

bunch in the first accelerator cavities Linac-1, the electron bunch acquires an RF curvature. Hence, a harmonic cavity Linac-X is introduced to compensate the curvature effect so to linearize the electron bunch and compress efficiently. The second BC2 then compresses the electron beam further down to $\sigma_z = 20 \mu\text{m}$. Complete and detailed design from cathode to the dump has been mostly finalized with only minor modifications for some concrete engineering design requests. The twiss parameters for the entire beam line is shown in Fig. 5. The evolution of the longitudinal phase space is shown in Fig. 6. Notice that, the final longitudinal distribution is a double-horn structure.

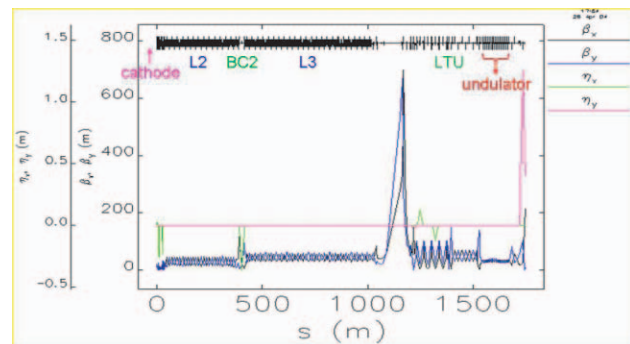


Figure 5: The twiss parameters for the LCLS beamline.

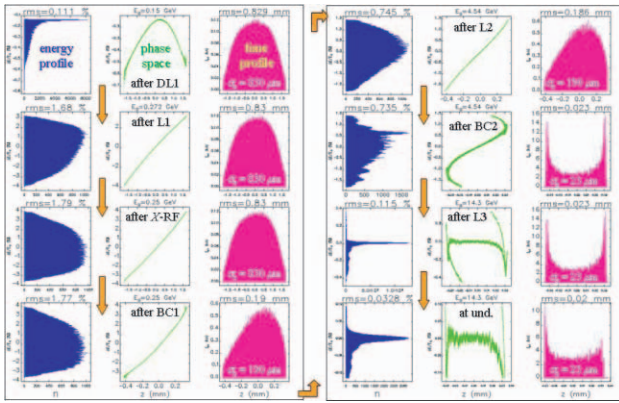


Figure 6: The evolution of the longitudinal phase space of the LCLS electron bunch along the beamline.

LINAC PHYSICS AND TECHNIQUE REQUIREMENT

The FEL lasing requires a set of very stable electron bunch parameters. However, in the LINAC, the elements can jitter. The low frequency deviation can be corrected by transverse and longitudinal feedback systems; yet, the high frequency jitter has to be minimized to meet the tolerance budget. According to FEL simulation, undulator trajectory oscillation of 35 mm ($1\sigma_x$) leads to about 30 % FEL power loss. Oscillation of 3.5 mm leads to 0.5 %. Hence, the total jitter goal we set is that the oscillation to be around 10 % of the rms beam size. In the following, the requirements on the possible jitter sources will be derived, and the feedback system will be described. To achieve this challenges, conventional and time-resolved diagnostics are needed. Due to the high field in the gun, and also in some structure component, there will be dark current forming the halo electrons travelling through the beamline together with the primary beam. Collimation system has to be designed to clean these halo particles. In the following, details of the LINAC physics and technique requirements will be illustrated.

Trajectory Jitter and Tolerances

In the LCLS operation mode, the machine will be running at 120 Hz. Beam based feedback system will be pulse-to-pulse, and effective for damping deviations with frequency lower than 10 Hz. For jitter with frequency higher than 10 Hz, the beam-based feedback system will be ineffective. Hence, we have to form a jitter tolerance budget to meet the tight requirement.

Any jitter of the element in the LINAC, will cause position and angular jitter on the electron trajectory. To characterize such jitter, the normalized invariant amplitude per element is the quantity to be examined. For the i^{th} element, the normalized invariant reads, $A_i = \sqrt{\frac{y_i^2 + (y_i\alpha_i + y_i'\beta_i)^2}{\epsilon_i\beta_i}}$, where $y_i(y_i')$ is the position (angular) jitter, α_i and β_i are the twiss parameters, and ϵ_i is the geometric emittance. Similarly, for the x -plane. Notice that the invariant has

been normalized to the beam size. For total of N elements, assuming no correlations among them, the total amplitude is then $A_T^2 = \sum_{i=1}^N A_i^2$. As we mentioned above, the total jitter goal we set is the random oscillation amplitude to be smaller than 10 % of the beam size, i.e., $A_T < 0.1$. We now ready to introduce the sensitivity $\sigma_{s,i}$ at each element. Assuming none but one element has jitter, which introduces an oscillation. If the oscillation due to this jitter is already 10 % of the rms beam size, then we define the rms value of this jitter as the sensitivity $\sigma_{s,i}$ of this element. Given total of N elements, and the sensitivity of each element, the most straightforward tolerance budget is to set the tolerance of each element to be $1/\sqrt{N}$ of the sensitivity. However, examining the elements in the LCLS LINAC system, we find that some of the elements are much more sensitive than others. Therefore, we form budget with a few discrete tolerance levels, to open challenging tolerances but hold tight on more standard ones. With three tolerance levels, we have $A_T^2 = 0.1^2 \left[\sum_{i=1}^{N_1} \left(\frac{\sigma_{t1}}{\sigma_{s,i}} \right)^2 + \sum_{i=1}^{N_2} \left(\frac{\sigma_{t2}}{\sigma_{s,i}} \right)^2 + \sum_{i=1}^{N_3} \left(\frac{\sigma_{t3}}{\sigma_{s,i}} \right)^2 \right]$, with $N_1 + N_2 + N_3 = N$, and σ_{t1} , σ_{t2} , and σ_{t3} are the three tolerance levels. With the above described approach, one can then examine each element in the LINAC system, identify jitter source, and set the tolerance budget. Such a budget and sources of jitter are summarized in Table 2. Seven sources of jitter are identified: Steering coils current jitter, trim coils current jitter; misaligned quadrupole current jitter (assuming rms misalignment $\Delta = 200 \mu\text{m}$), quadrupole / solenoid mechanical vibration, transverse wakefield due to misalignment couples to charge jitter (assume rms misalignment $\Delta = 200 \mu\text{m}$), Coherent Synchrotron Radiation (CSR) couples to bunch length jitter, and drive laser pointing jitter. As one can readily see, the largest kicks come from the CSR issue as in Fig. 7. Summing up all the jitter sources, the total normalized oscillation amplitude is about 24 % in the x -plane, and 13 % in the y -plane [2].

Table 2: Sources of jitter and tolerance budget. The rms misalignment is taken as $\Delta = 200 \mu\text{m}$.

Sources	Tolerance	A (%)
Steering coils current	30-100 ppM	6
Trim coils current	30-100 ppM	2
Misalg. quads cur. with Δ	25-100 ppM	5
Quad/solenoid vib.	0.05-1 μm	10
Trans. Wakes with Δ	$\frac{\Delta N}{N} = 2 \%$	2
CSR kicks (1 nC)	$\frac{\Delta\sigma_z}{\sigma_z} = 10 \%$	20 (x)
Drive laser pointing		3

Feedback System

To maintain stable performance, a feedback system is mandatory for the LCLS. The transverse feedback system will be based on what has been developed for the SLAC Linear Collider, even though it will mitigate to the EPICS system. We will not discuss such a transverse feedback system, but focus on the longitudinal feedback system [3].

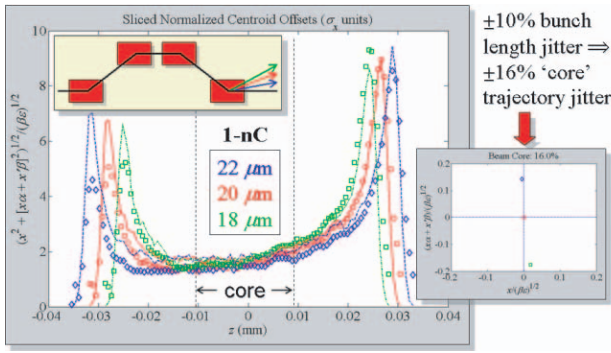


Figure 7: The CSR coupling to the bunch length jitter generate large trajectory jitter.

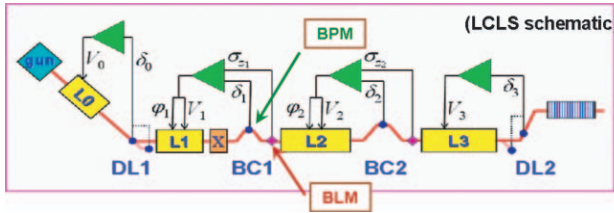


Figure 8: Schematics of the LCLS longitudinal feedback.

In such a longitudinal feedback system, there are 6 observables: energy E_0 (at DL1), E_1 (at BC1), E_2 (at BC2), E_3 (at DL2); and electron bunch length $\sigma_{z,1}$ (at BC1), $\sigma_{z,2}$ (at BC2). Then there are 6 controllables: voltage V_0 (in L0), V_1 (in L1), V_2 (effectively, in L2); and phase φ_1 (in L1), φ_2 (in L2), and φ_3 (in L3). The energy will be measured by Bunch Position Monitors (BPMs) installed in DL1, BC1, BC2, and DL2, and the bunch length by Bunch Length Monitors (BLMs) right after BC1 and BC2. The feedback algorithm is simply PID scheme.

Based on measurement of jitter from the SLAC LINAC, the simulation results are shown in Fig. 9. Recalled that the tolerance budget requires that $|\langle \Delta E/E_0 \rangle| < 0.1\%$ and $|\Delta I/I_0| < 12\%$. Hence, the longitudinal feedback system can maintain the system parameters within the specifications. Indeed, the longitudinal feedback model simulation can be used as a measure of the tolerance budget. This model simulation points to $dV/V = 0.1\%$ and $d\varphi = 0.1^\circ$ (S-band) as the tolerance on the RF-jitter.

Diagnostics

Both the conventional and time-resolved diagnostics will be installed to help meet the tight tolerance budget. The diagnostic package in the injector is shown in Fig. 10, while the diagnostic package for the main LINAC is shown in Fig. 11. In the main LINAC, there are more than 5 energy spread measurement stations (optimized with small β -function); more than 5 emittance measurement stations designed into optics ($\Delta\Psi_{x,y}$); BPMs at or near most quadrupoles and in each bend system; and RF deflectors for slice emittance and slice energy spread measurements

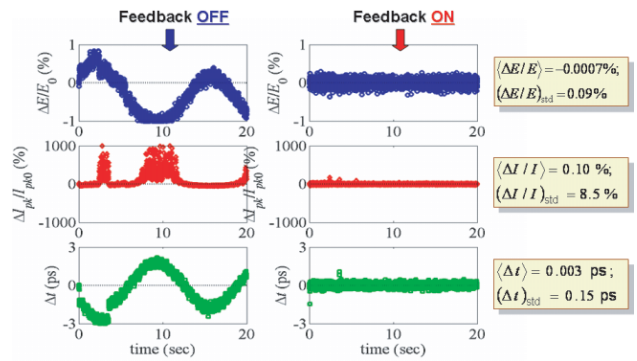


Figure 9: Simulation of the longitudinal feedback system.

(L0 and L3). A schematic plot of a transverse deflecting cavity is shown in Fig. 12. A transverse deflecting cavity is also the ultimate tool to measure the bunch length. The other relative bunch length monitor is shown in Fig. 13. It is based on the coherent radiation power from the last bending magnet of the bunch compressors [4, 5]. The optics is designed to focus on the exit edge of the bending magnet. So, mostly the signal is the near field edge radiation from the exit edge of the last bending magnet [5].

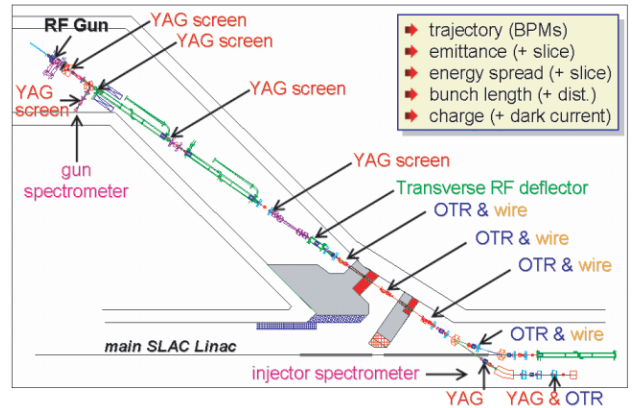


Figure 10: The diagnostic package in the LCLS injector.

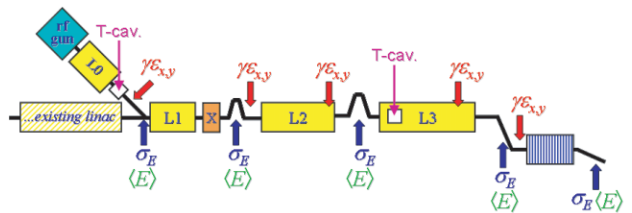


Figure 11: The diagnostic package in the LCLS LINAC.

Collimation System

In the LCLS gun, the peak field is as high as $E_{RF} = 120$ MV/m. Hence, substantial dark current is generated. This dark current forms the halo electrons when it travels downstream with the primary electron bunch. We model

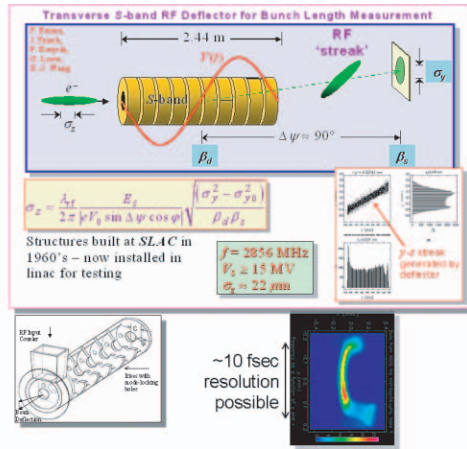


Figure 12: The transverse deflecting S-band cavity.

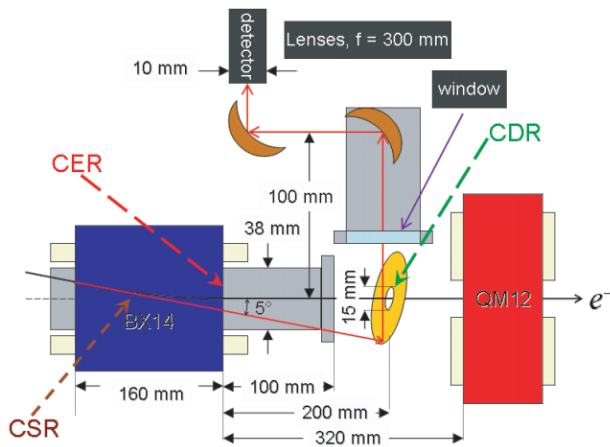


Figure 13: The schematic layout of the coherent radiation based BLM (BL11) after BC1.

this dark current following the “Fowler-Nordheim” model with normalization against experimental data as shown in Fig. 14. Besides the dark current from the gun, there is also dark current generated from the LINAC cavities. This dark current is less severe since it has too low energy compared with the primary electron bunch, hence gets lost locally. To protect the very precise magnet field of the undulator magnet, we have to design collimator system upstream of the undulator, so that no halo electron will hit the undulator wall. This is done by introducing new collimators together with the existing collimators. Locations of the collimators, and particle losses through the undulator and dump is shown in Fig. 15. With this design, based on the simulation, none of the halo electrons will hit the undulator wall [6].

DISCUSSION

Stability has been studied for the LCLS accelerator system to form the tolerance budget. Based on the study, the trajectory oscillation amplitude will be 24 % (x -plane) and

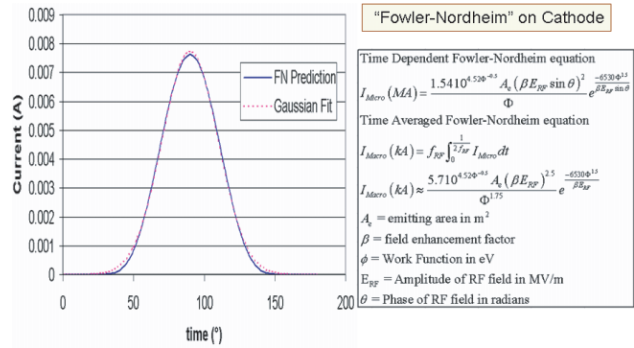


Figure 14: Dark current generation at the cathode following “Fowler-Nordheim” model.

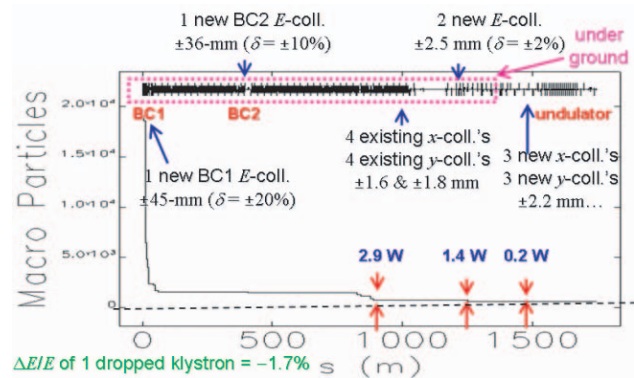


Figure 15: Locations of the collimators, and particle losses through undulator and dump.

13 % (y -plane) of rms beam size for the 1 nC charge operation mode. With 0.2 nC, the oscillation amplitude is much smaller. The feedback systems have been designed, and being implemented into the LCLS control system. Such a feedback system requires a Coherent Radiation based relative bunch length monitor. Conventional and time-resolved diagnostics package has been planned for the LCLS injector and main LINAC. Beam collimation systems have been designed. Such a collimation system protects the undulator from gun and structure dark current. Maximum collimated beam power is 0.2 W above ground. Collimator wakes should not be an issue. Commissioning plans have been formed. Installation of injector through first bunch compressor will complete by December 2006, and electron commissioning is scheduled to begin in January 2007.

REFERENCES

- [1] J. Arthur *et al.*, SLAC-R-593, 2002.
- [2] P. Emma *et al.*, EPAC-06, p. 151, Edinburgh, Scotland, 2006.
- [3] J. Wu *et al.*, PAC-05, p. 1156, Knoxville, TN, 2005.
- [4] J. Wu *et al.*, PAC-05, p. 428, Knoxville, TN, 2005.
- [5] J. Wu *et al.*, LINAC-06, this proceedings, Knoxville, TN, 2006.
- [6] P. Emma *et al.*, EPAC-06, p. 148, Edinburgh, Scotland, 2006.